
Article:
Ghorani, B, Goswami, P orcid.org/0000-0003-1488-409X, Blackburn, RS orcid.org/0000-0001-6259-3807 et al. (1 more author) (2018) Enrichment of cellulose acetate nanofibre assemblies for therapeutic delivery of L-tryptophan. International Journal of Biological Macromolecules, 108. pp. 1-8. ISSN 0141-8130

https://doi.org/10.1016/j.ijbiomac.2017.11.124

Enrichment of cellulose acetate nanofibre assemblies for therapeutic delivery of L-tryptophan

Behrouz Ghorani,[a,b] Parikshit Goswami,[c] Richard S. Blackburn,[a] Stephen J. Russell[a*]

[a]Textile Technology Group, School of Design, University of Leeds, Leeds, LS2 9JT, UK.

[b]Department of Food Nanotechnology, Research Institute of Food Science and Technology (RIFST), Km 12 Mashhad-Quchan Highway P.O. Box: 91895/157/356, Mashhad, Iran.

[c]Department of Fashion and Textiles, University of Huddersfield, Huddersfield, HD1 3DH, UK.

Corresponding Author:*S. J. Russell, Textile Technology Group, School of Design, University of Leeds, Leeds, LS2 9JT, UK. E-mail: s.j.russell@leeds.ac.uk; Phone: +44 (0)113 343 3700.

Abstract

The essential amino acid L-tryptophan is naturally present in the body, and is also available as a water soluble dietary supplement. The feasibility of preparing enriched cellulose acetate (CA)-based fibres as a vehicle for therapeutic delivery of such biomolecules was investigated. A new ternary solvent system consisting of acetone: N,N-dimethylacetamide: methanol (2:1:2) has been demonstrated to permit the solution blending of CA with the water soluble L-tryptophan. Nanofibrous webs substantially free of structural defects were continuously produced with mean fibre diameters in the range of 520-1,010 nm, dependent on process parameters. Morphology and diameter of fibres were influenced by concentration of CA spinning solution, applied voltage and flow rates. The kinetic release profile of L-tryptophan from electrospun CA nanofibres was described by the pseudo-second order kinetic model. Fibres with mean diameter of 720 nm provide both the highest initial desorption rate and rate constant, which was partially attributed to the low fibre diameter and high relative surface area, but also the fact that the fibres with mean diameter of 720 nm produced were the most bead-free, providing diffusion advantages over the fibres with lowest mean diameter (520 nm). The feasibility of combining L-tryptophan within fibres provides a promising route for manufacture of transdermal delivery devices.

Keywords: electrospinning; cellulose acetate; nanofibres; amino acid; tryptophan

1. Introduction

Cellulose acetate (CA) fibres and membranes have important biomedical applications in affinity membranes and drug delivery [1]. The development of experimental biomedical products continues to involve solution blending of the polymer with other therapeutic molecules and compounds. Research has led to the fabrication of various functional materials including antibacterial CA nanofibres containing $AgNO_3$ [2], nanofibres for therapeutic delivery of active compounds, such as vitamins A and E [3], curcumin [4], nicotine [5], naproxen [6], gallic acid [1], gingerol [7], tetracycline hydrochloride [8], ketoprofen [9], the assembly of topical drug delivery carriers containing non-steroidal anti-inflammatory drugs (NSAIDs) [10], and edible nanofibrous films containing egg albumen [11].

One of the most versatile solvent systems for electrospinning of CA is a binary system of acetone: N,N-dimethylacetamide (DMAc) (2:1) incorporating 12.5-20.0 wt.% CA [12,13]. The use of such binary solvent systems has been utilised by various researchers to optimise the electrospinning process, for example, achieving high productivity concurrently with a finer fibre diameter. Van der Schueren et al. [14] showed that substantial reduction of the cross-sectional area of electrospun fibres could be achieved by selecting a binary rather than single solvent system. In addition to improving spinning performance and tuning fibre dimensions, mixed solvent systems have also been found to assist in the production of nanofibres from blended compositions containing a fibre forming polymer and functional compounds; Ma et al. [15,16] reported the development of a ternary system of acetone: N,N-dimethylformamide (DMF): trifluoroethanol (3:1:1) for the preparation of protein A/G functionalised CA membranes. In another approach, CA fibres loaded with the ester prodrugs of Naproxen (including methyl, ethyl, and isopropyl esters) were prepared by electrospinning using a mixed solvent of acetone: DMAc: ethanol (4:1:1) [6].

L-tryptophan (**1**) is an essential amino acid naturally present in the body and is commercially available as a dietary supplement. Brain serotonin (5-HT) synthesis and release due to L-tryptophan depletion has been linked with depression, insomnia, migraines and bulimia with minimum levels of intake being advised [17]; as such, a novel therapeutic delivery method for L-tryptophan is desirable. Production of CA fibres containing water soluble biomolecules requires selection of a compatible co-solvent; however, the solubility of highly polar amino acid molecules is low in single organic solvents routinely used for CA electrospinning. Previous attempts to solution blend CA with therapeutic drugs such as Naproxen, Indomethacin, Ibuprofen, Sulindac and curcumin have relied up on solvent systems of acetone: DMAc (6:4) [18], however, such a system is not suitable for spinning highly polar molecules such as L-tryptophan.

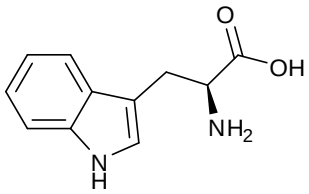

1

Ultrafine CA fibres have been successfully produced via electrospinning of CA in a mixed solvent of acetone: water incorporating 10-15 wt.% of polymer [19]; electrospinning of a CA solution in acetone and water under acidic conditions produced larger fibres; a basic solution produced much finer fibres. Tungprapa et al. [13] reported that both beaded and smooth fibres can be electrospun at CA concentration of 16 wt.% in mixed solvent systems of chloroform: methanol using ratios of the mixed solvents from 9:1 to 3:2 v/v. The average diameter of these fibres varied from 520 nm to 1,090 nm.

Owing to their polarity, many previously reported binary and ternary solvent systems for CA are not suitable for co-spinning with polar biomolecules such as L-tryptophan [12,13,15,16,20-22]. Herein we report the development of alternative binary and ternary solvent systems enabling incorporation of L-tryptophan in electrospun CA nanofibres, characterisation of resulting nanofibre webs, and diffusion kinetics of L-tryptophan from prepared fibres.

2. Material and Methods

2.1. Materials

Cellulose acetate (acetyl content 39.8% w/w, M_w 30,000 Da), L-tryptophan (99.5%), and all solvents (HPLC grade) were purchased from Sigma-Aldrich.

2.2. Sample preparation

Solvents were prepared in binary and ternary compositions based on existing literature [13,19] and novel binary and ternary solvent systems (Table 1). Solutions were prepared by constant stirring at room temperature (25±5 °C). CA concentration in the spinning solutions was fixed at a concentration of 13% w/v; this concentration was selected based on previous studies to establish the most suitable solvent systems [12,20]. The suitability of each system was assessed in terms of the freedom from precipitation during preparation of the spinning solution and the spinability of the resulting polymer solution. Spinability in this context was assessed in terms of freedom from needle blockages, consistency of fibre morphology, and freedom from bead and spindle defects in the web.

Clear spinning solutions were obtained after 24 h. To prepare spinning solutions of L-tryptophan in a ternary acetone: DMAc: methanol solvent system, a fixed concentration of L-tryptophan was pre-dissolved in 20 ml of methanol before incorporation into the spinning solutions, which comprised 13% w/v CA in acetone: DMAc: methanol (2:1:2). Solutions were stirred for 5-7 hrs at ambient temperature.

2.3. Electrospinning

Electrospinning was performed in horizontal alignment with the polymer solution loaded into a 5 ml syringe (Fortuna and Graff) connected to a blunt-ended Luer lock metal needle (20 gauge, Sigma-Aldrich). The syringe was mounted into a syringe pump (KD Scientific) connected to a high voltage power supply (Glassman Inc.). Electrospinning was performed inside a fume cupboard under ambient conditions at an applied voltage of 20-30 kV and a tip-collector distance of 130 mm. The spinning solution feed rate was varied between 0.002-0.004 ml min^{-1}. Flat aluminium foil collectors were used throughout.

2.4. Scanning electron microscopy and image analysis

Samples were sputter coated then imaged with a field emission scanning electron microscopy (SEM) (Camscan series 4 environmental) to observe the fibre morphology and web structure. Mean fibre diameters in the collected webs were determined directly from the SEM images by image analysis (Media Cybernetics, Image Pro-Plus 7) by measuring the diameter of 50 individual fibres. To estimate the porosity (P) in the webs, binary SEM images (bitmap format) were prepared by image thresholding techniques and determined from the mean intensity of the image according to equation 1:

$$P = \left(1 - \frac{n}{N}\right) 100 \quad (1)$$

where n is the number of white pixels and N is the total number of pixels in binary image [23,24].

2.5. Spectrophotometry

UV spectrophotometric analysis was conducted using a Jasco V-630 spectrophotometer in the UV and visible regions of the spectrum (190-700 nm), at 1 nm intervals. The solutions were diluted using distilled water and measured at the wavelength of maximum absorption (λ_{max}) for L-tryptophan, which was determined to be 280 nm. No difference in the shape of the absorption spectrum before and after incorporation or upon diffusion was noted. UV absorption calibration curves for L-tryptophan were obtained at 280 nm. To determine the polar molecular content,

nanofibre webs were peeled off the collector and a fixed mass of each sample was added to 50 ml of distilled water and shaken at a constant temperature of 37 °C for 1 hr.

2.6. L-Tryptophan Encapsulation Efficiency

To determine the concentration of L-tryptophan loaded in nanofibres (m_{fibre}), the specific weight of each electrospun sample was suspended in 50 ml of deionised water (pH 6.2) and then shaken in a water bath at room temperature (25±5 ºC); the resulting solution was analysed by UV at 280 nm in triplicate and the concentration determined from calibration graphs. Encapsulation efficiency (EE) was calculated using equation 2 [25]

$$EE(\%) = 100\frac{m_{fibre}}{m_{formulation}} \quad (2)$$

where $m_{formulation}$ is the concentration of L-tryptophan loaded into the initial formulation use to produce the nanofibres.

2.7. L-Tryptophan release kinetics

CA samples were prepared at different concentrations (10-20% w/v) and a fixed amount of L-tryptophan. The release of L-tryptophan from the webs was determined by introducing a sample of nanofibre web into 50 ml deionised water at pH 6.2 and orbitally shaken for 60 min at room temperature (25±5 ºC). The release was monitored at 280 nm as a function of time; equilibrium was obtained after 4 hr. Release monitoring experiments were done in triplicate. To determine the effect of fibre diameter, three samples at a fixed CA concentration (14% w/v) with different mean fibre diameters were used and the diffusion of L-tryptophan assessed. 150 mg of each electrospun sample was suspended in 50 ml of deionised water (pH 6.2) and was then shaken in a water bath at room temperature (25±5 ºC) and the resulting solution analysed by UV spectrophotometry. The ratio of L-tryptophan/polymer content (%) in the web was also measured before and after the electrospinning process following 60 min immersion in water.

3. Results and Discussion

L-tryptophan is soluble in water and methanol, slightly soluble in ethanol and is practically insoluble in chloroform and ether [17,26], hence, achieving dissolution in conventional solvents for

CA electrospinning is challenging. Accordingly, binary and ternary solvent systems containing methanol as the major component were evaluated to identify polar spinning solutions suitable for electrospinning of co-mixtures of CA and L-tryptophan; the purpose of this initial work was to verify the feasibility of producing nanofibres free of beads and defects before adding the L-tryptophan component. A comparative evaluation using mixed solvents containing methanol was conducted, based on some literature examples [13,20] and novel systems developed herein. Spinning solutions were prepared for each combination, using a constant CA polymer concentration of 13% w/v. It was found that electrospinning of CA from a mixed acetone: water (4:1) system, as previously described [19], could not be satisfactorily reproduced (Table 1). The solubility of CA in methanol: acetone is affected by relative concentration, and it was observed that in a single solvent system [20] or binary solvent systems of ratios of 3:2 to 4:1, satisfactory spinning conditions could not be established and continuous electrospinning was hampered by the low boiling points of both solvents. Increasing the proportion of acetone improved spinning stability and resultant fibres were substantially bead-free and formed with diameters in the range of 435-1,010 nm. For the other mixed solvents, fibrous webs were satisfactorily produced on a continuous basis for up to 1 h. Typical resulting web structures are shown in Figure 1 with dimensional properties given in Table 1.

Table 1. Measured CA fibre diameter (nm) and fabric porosity from mixed-solvent systems. Spinning solutions were prepared for each combination, using a constant CA polymer concentration of 13% w/v.

Solvent System	**Ratio of mixed solvent (v/v)**	**Mean fibre diameter (nm)**	**Porosity (%)**
acetone: water [19]	4:1	No production	No production
chloroform: methanol [13]	4:1	1,100	70
methanol: acetone	3:2 to 4:1	No production	No production
acetone: methanol	3:2	1,010	76
acetone: methanol	4:1	435	68
acetone: DMAc: methanol	2:1:2	710	63
acetone: DMF: methanol	2.67:1.33:1	570	64
acetone: DMF: methanol	3:1:1	590	59

Mean fibre diameter, morphology and bead formation varied depending on the solvent system. Mean fibre diameter in the collected webs was ≤710 nm, except for those produced from the acetone: methanol (4:1) spinning solution, where mean fibre diameter was 435 nm, acetone: methanol (3:2) spinning solution, where mean fibre diameter was 1,010 nm, and chloroform: methanol (4:1) spinning solutions, where mean fibre diameter was 1,100 nm. With respect to fibre morphology, ribbon and tape forms were observed to varying extents in the webs produced from acetone: methanol (3:2) (Figure 1a), acetone: methanol (4:1) (Figure 1b), and chloroform: methanol (4:1) (Figure1c; SEM shown in Figure 2 demonstrating collapsed ribbon-like form). Tubular, collapsed ribbon, tape, branched and various other forms are frequently observed in electrospun fibres depending on solvent properties, spinning solution rheology and process conditions [20, 27]. Rapid evaporation and diffusion of solvent and the presence of a thin, mechanically distinct polymer skin on the surface of the liquid jet, leads to collapse of the tubular morphology at atmospheric pressure [20]. Previously, experimental studies have indicated that the cross-sectional perimeter of the resulting ribbon can be expected to be of similar dimensions as the liquid jet [20,27]. In addition to inconsistent fibre morphologies, spinability issues were encountered due to rapid evaporation of chloroform at the nozzle tip leading to blockage.

Fibre morphology and spinability can be explained in terms of the relative solvency of the different solvent components [21]; in addition to the initial viscosity of the polymer solution, rapid evaporation of the most volatile solvent component during electrospinning can lead to an increase in viscosity as well as to variation in the dissolution capability of the solvent. Accordingly, the solubility range of a mixed binary or ternary solvent system is therefore of greater interest than the maximum solubility [20,21]. Smooth fibre morphologies, substantially free of beads, were evident in webs produced from the ternary system of acetone: DMAc: methanol (2:1:2), with an observed mean fibre diameter of 710 nm (Figure 1d). By contrast, a high incidence of bead formation was observed in the ternary system of acetone: DMF: methanol (2.67:1.33:1) (Figure 1e) and acetone: DMF: methanol (3:1:1) (Figure 1f). During electrospinning, Rayleigh instability in the polymer jet can result in fragmentation and the formation of droplets and subsequently beads in the collected web rather than continuous fibres [21,28]. Since solution concentrations are below the dilute solution regime, polymer chain overlap is not enough for electrospinning solutions and appreciable interactions among molecules [28]. As a result, uniform microbeads generate through the nanofibre structure due to limiting chain entanglements [29-31]. Increasing chain entanglement by increasing polymer concentration can temporarily serve to stabilise the electrospinning jet by inhibiting jet break up and decreasing bead formation.

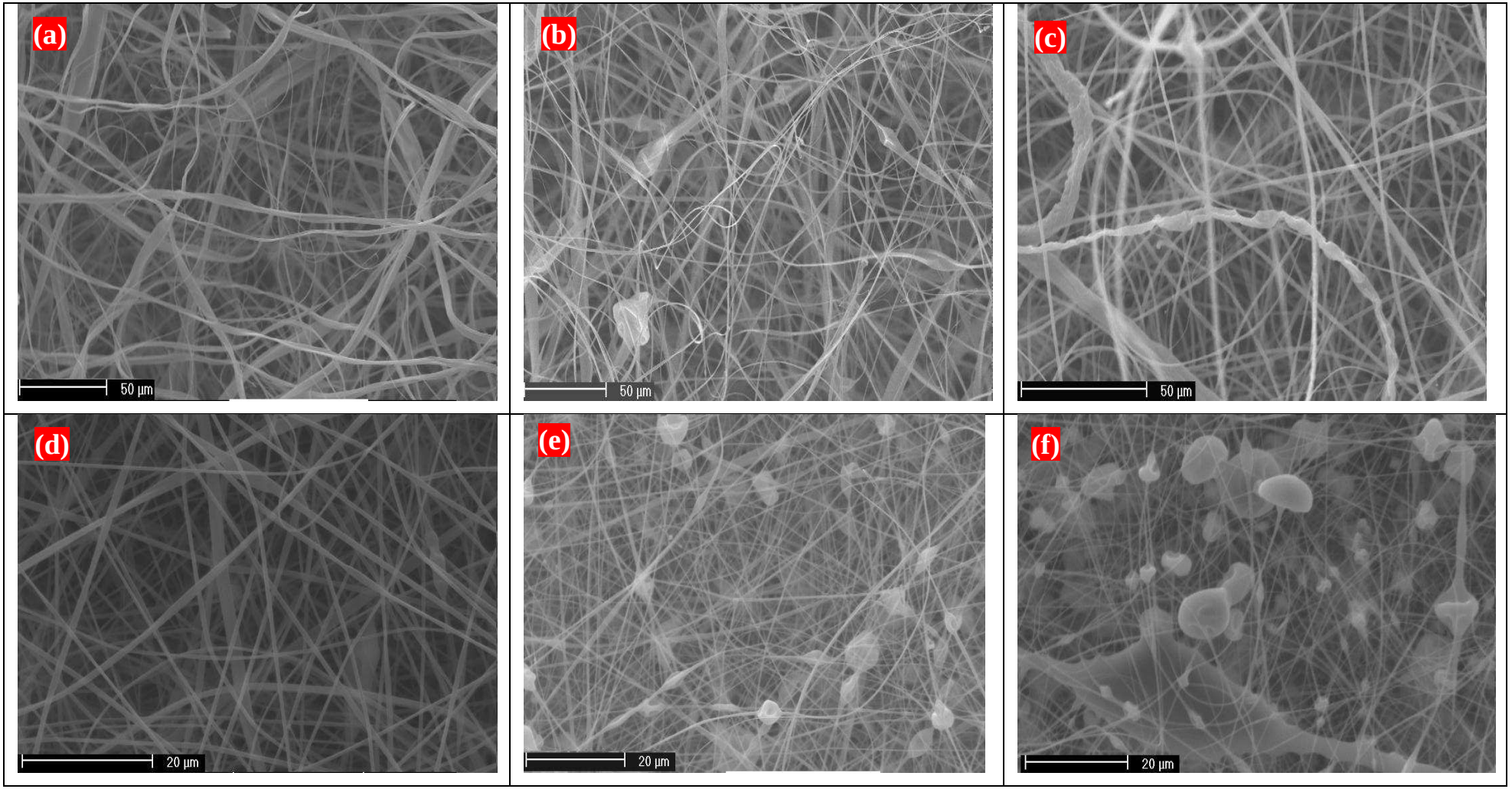

Figure 1. SEM micrographs showing the effect of binary and ternary solvent systems containing methanol on the structure and morphology of resulting CA electrospun webs. Spinning solutions were prepared for each combination, using a constant CA polymer concentration of 13% w/v. Magnification x630 to x1260: (a) acetone: methanol (3:2); (b) acetone: methanol (4:1); (c) chloroform: methanol (4:1); (d) acetone: DMAc: methanol (2:1:2); (e) acetone: DMF: methanol (2.67:1.33:1); (f) acetone: DMF: methanol (3:1:1).

Furthermore, polymer-polymer interactions are not significant enough to affect solution viscosity, thus addition of another solvent can dramatically alter the concentration needed for fibre formation without any beads on the surface [28,31]. Note that by controlling molecular weight and concentration, various bead morphologies, including wrinkles, beads, cups, dishes, etc., may be obtained [31].

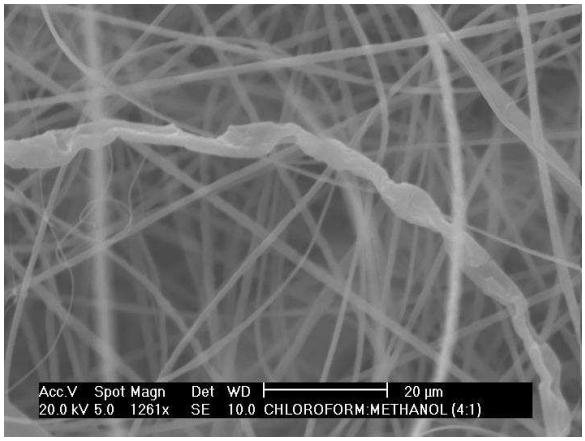

Figure 2. SEM micrograph of collapsed ribbon-like CA fibre produced from chloroform: methanol (4:1).

Given the promising results obtained when spinning CA from a ternary system of acetone: DMAc: methanol (2:1:2), this novel solvent system was selected for further experiments with L-tryptophan loading. Successful production of CA/L-tryptophan fibres was achieved with average fibre diameter of 640±20 nm and the porosity of nanofibre web of 50-60% (Figure 3). The presence of the L-tryptophan in the CA nanofibres was confirmed by UV spectrophotometry; measurement of L-tryptophan concentration at 280 nm clearly indicated that 79% of the pre-loaded L-tryptophan was released in water after 60 min.

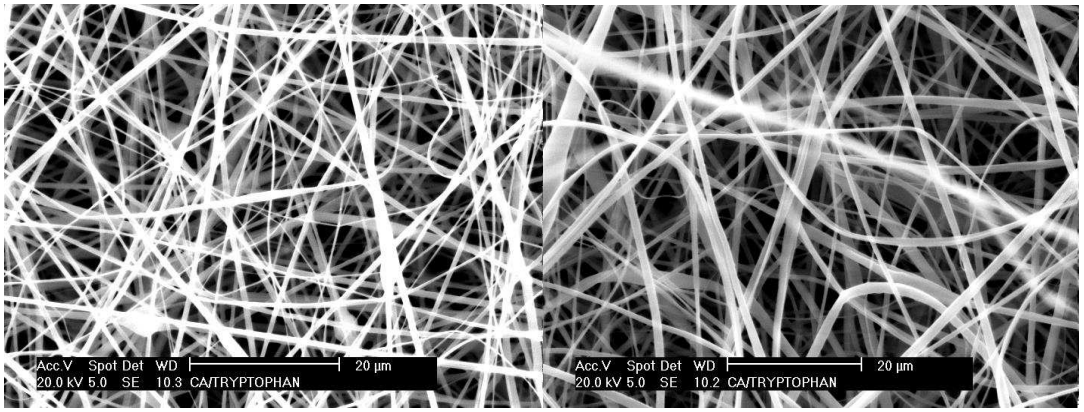

Figure 3. SEM micrographs of CA/L-tryptophan webs produced from ternary mixed solvent systems acetone: DMAc: methanol (2:1:2). Mean fibre diameter = 640 nm; porosity = 56%.

To investigate the effect of polymer concentration and fibre diameter on the rate of diffusion, CA samples made with different polymer concentrations (10-20% w/v) and fixed amounts of L-tryptophan were prepared. The optimal CA concentration was 14%-16% w/v as judged by the ability to produce bead-free fibres using the ternary system of acetone: DMAc: methanol (2:1:2) (Figure 4); some evidence of bead formation was observed at 12% w/v. No fibres were produced at a concentration of 10% w/v due to the dilute solution and low viscosity. Similarly as the concentration approached 20% w/v, formation and elongation of the jet was impossible due to the high viscosity of solvent in the applied electric field (20-30 kV), consequently, the solvent had insufficient time to evaporate and large elongated beads were formed. At a polymer concentration of 18% w/v, fibre production was inconsistent, although the morphology of fibres that were produced showed little evidence of bead defects (Figure 4d). Subsequently, all the experiments were conducted with concentrations of 12-16% w/v. As expected, average fibre diameter increased due to increasing polymer concentration (Table 2).

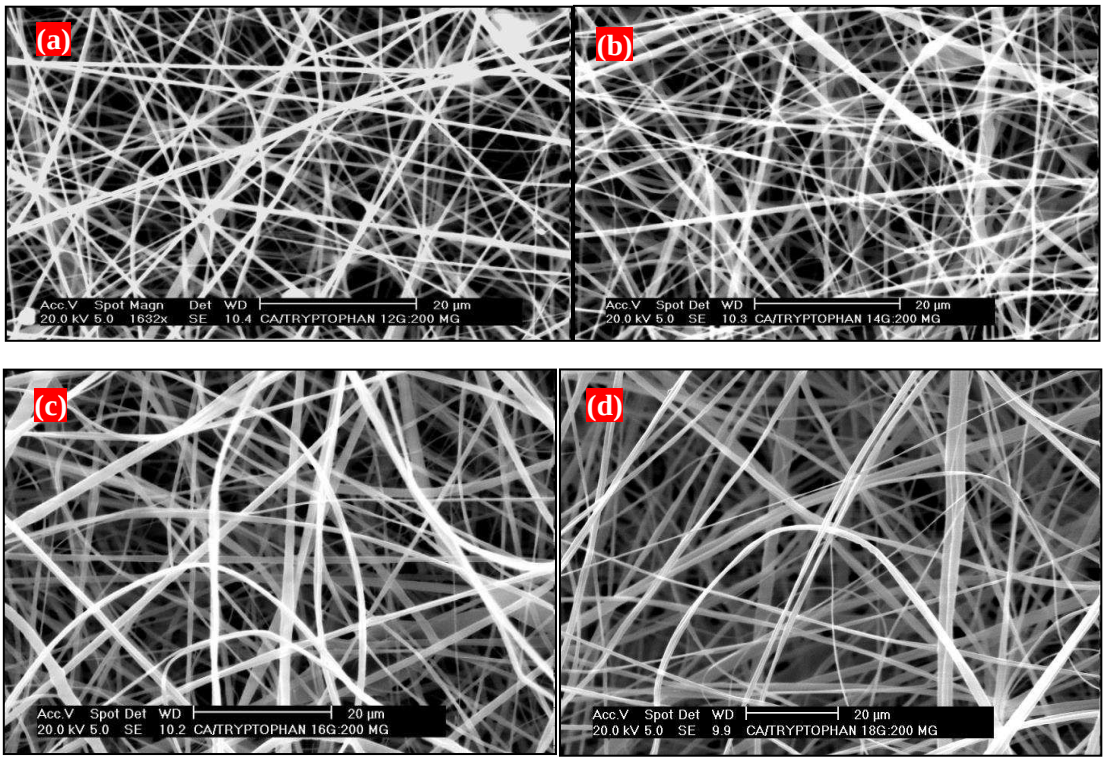

Figure 4. Selected SEM micrographs of electrospun CA/L-tryptophan webs produced with different CA concentrations: (a) 12% w/v CA; (b) 14% w/v CA; (c) 16% w/v CA; (d) 18%w/v CA. All were produced from a ternary mixed solvent system of acetone: DMAc: methanol (2:1:2).

Table 2. Measured CA fibre properties from a ternary mixed solvent system of acetone: DMAc: methanol (2:1:2) with L-tryptophan content and encapsulation efficiency for each sample.

CA loading in spinning solution (%w/v)	Resultant mean fibre diameter (nm)	Web porosity (%)	Encapsulation efficiency (%)	L-tryptophan content (mg/g of fibre)
12	580	53	86	2.18
14	720	57	82	1.79
16	1,010	64	85	1.61
18	1,820	60	N/A	N/A

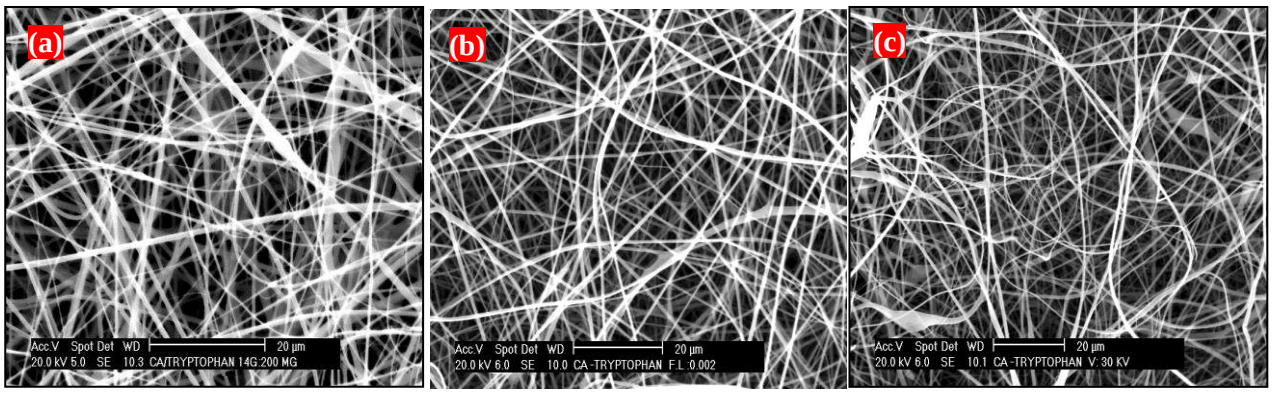

Figure 5. SEM micrograph of CA/L-tryptophan webs produced from ternary mixed solvent system acetone: DMAc: methanol (2:1:2) at 14% w/v CA: (a) flow rate: 0.004 ml min^{-1}, V: 25 kV; (b) flow rate: 0.002 ml min^{-1}, V: 25 kV; (c) flow rate: 0.004 ml min^{-1}, V: 30 kV.

Fibres were readily produced at a high rate of production when the CA concentration was 14% w/v, voltage was 25 kV and the flow rate was 0.002 ml min^{-1} (Figure 5b). However, at the higher flow rate of 0.004 ml min^{-1}, and as the voltage was progressively increased from 25 kV to 30 kV, some bead formation was in evidence (Figure 5a and 5c). Interestingly, mean fibre diameter of CA-tryptophan nanofibres was lower at the higher flow rate, although as the voltage increased to 30 kV, the average fibre diameter substantially increased (Table 3). This can be attributed to a shorter time for extension of the polymer stream during spinning of the CA-tryptophan solution [29]. Consequently, at a higher voltage, there is increased tendency for bead formation and higher fibre diameters [32].

Table 3. Measured CA fibre properties diameter from a ternary mixed solvent system of acetone: DMAc: methanol (2:1:2), combination, using a constant CA polymer concentration of 14% w/v.

Spinning flow rate (ml min^{-1})	Spinning voltage (kV)	Resultant mean fibre diameter (nm)	Web porosity (%)	Encapsulation efficiency (%)	L-tryptophan content (mg/g of fibre)
0.004	25	520	58	87	1.90
0.002	25	720	60	81	1.79
0.004	30	850	68	80	1.76

3.3. Kinetics

As shown in Tables 2 and 3, L-tryptophan loading efficiency was in the range 80-90%, demonstrating potential for high loading efficiencies [29,33]. The kinetic release profile of a fixed concentration of L-tryptophan from fibres with different initial concentrations of CA (12-16% w/v) is shown in Figure 6, where it is observed that after initial rapid rate of desorption, plateau eventually occurs with increasing time. The data was fitted to a pseudo-second order kinetic model [33-35] as described in equation 2:

$$\frac{dq_t}{dt} = -K_2(q_t - q_e)^2 \quad (2)$$

where q_e and q_t are the amounts of the compound released from the fibre web at equilibrium and at various times t (mg g^{-1}). The term, K_2 is the rate constant of the pseudo-second order equation (mg $g^{-1}min^{-1}$). For the boundary conditions t=0 to t=t and q_t=0 to q_t=q_t, the integrated form of equation (2) becomes equation 3:

$$\frac{t}{q_t} = \frac{-1}{K_2 q_e^2} + \frac{t}{q_e} \quad (3)$$

A plot of t/q_t against t that produces a straight line, confirms the model, wherein K_2 and q_e are determined from the intercept and slope of the plots respectively. Initial desorption rate h_0 (mg $g^{-1}min^{-1}$) is given by equation 4:

$$h_0 = K_2 q_e^2 \quad (4)$$

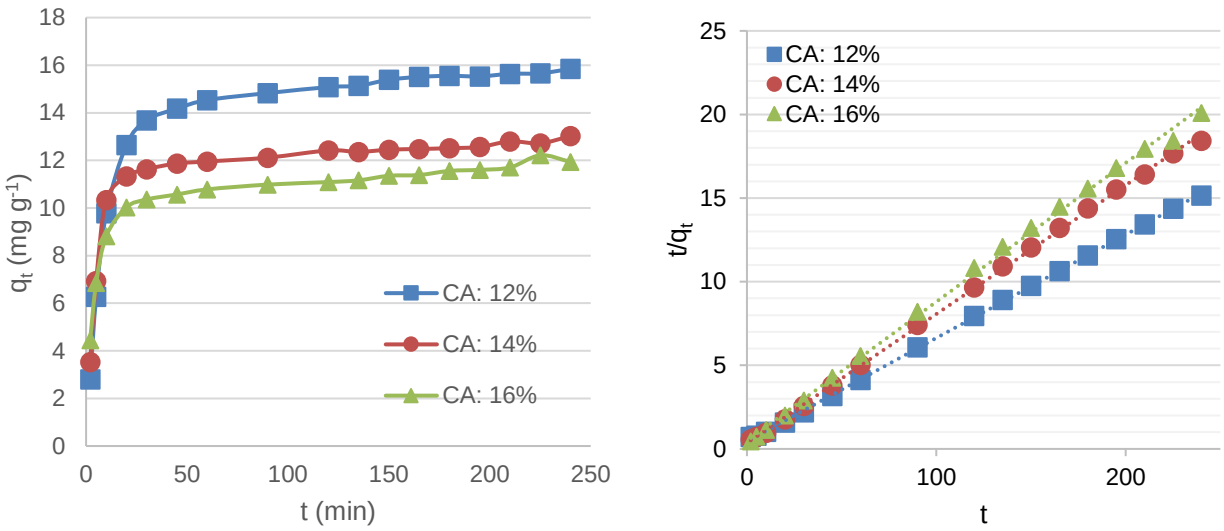

Figure 6. Left: Diffusion of L-tryptophan in water from the electrospun webs at different CA concentrations in solvent in preparation: (■) 12% w/v, mean fibre diameter = 580 nm; (●) 14% w/v, mean fibre diameter = 720 nm; (▲) 16% w/v, mean fibre diameter = 1.01 nm. Right: residual plots from application of pseudo-second order model (t/q_t vs. t).

Table 4 shows the kinetic data derived from diffusion data by application of the pseudo-second order kinetic model, where it is observed that the sample prepared with an initial CA spinning solution concentration of 14% w/v, with resultant fibres with a mean diameter of 720 nm, provide both the highest initial desorption rate (2.80 mg $g^{-1}min^{-1}$) and rate constant (0.0166 mg g^{-1} min^{-1}). The sample prepared with an initial CA spinning solution concentration of 12% w/v, with resultant fibres with a mean diameter of 580 nm, gives both the lowest initial desorption rate and rate constant, but provides the highest total desorption at equilibrium (q_e = 16.18 mg g^{-1}). The dimensional properties of the fibres and the web can be expected to influence release behaviour and the length of the diffusion pathway [36,37]. Another factor relates to the distribution of the diffusing molecule within the fibres, and the proximity to the fibre surfaces, therefore, increases in fibre diameter are likely to result in longer diffusion pathways and a slower rate of delivery. In all samples, release was greatest during the initial period after immersion, because of rapid diffusion of L-tryptophan from the fibre surfaces [6,38].

Table 4. Data for the pseudo-second order kinetic model applied to diffusion of L-tryptophan in water from the electrospun webs with varying CA concentration in initial spinning solution.

CA (% w/v)	Mean fibre diameter (nm)	q_e (mg g^{-1})	$-h_0$ (mg g^{-1} min^{-1})	$-K_2$ (mg g^{-1} min^{-1})	R^2
12	580	16.18	2.21	0.0085	1.000
14	720	12.97	2.80	0.0166	0.999
16	1,010	12.03	2.04	0.0141	0.998

Figure 7 shows desorption behaviour of L-tryptophan from electrospun webs with varying fibre diameter where all samples were prepared with an initial CA solution concentration of 14% w/v. Table 5 shows the kinetic data derived from diffusion data by application of the pseudo-second order kinetic model for all samples prepared with an initial CA spinning solution concentration of 14% w/v. It is observed that fibres with a mean fibre diameter of 720 nm, provide both the highest initial desorption rate (4.84 mg g^{-1} min^{-1}) and rate constant (0.0096 mg g^{-1} min^{-1}); fibres with a mean fibre diameter of 850 nm give both the lowest initial desorption rate and rate constant. Total desorption at equilibrium is essentially equal within error for all samples.

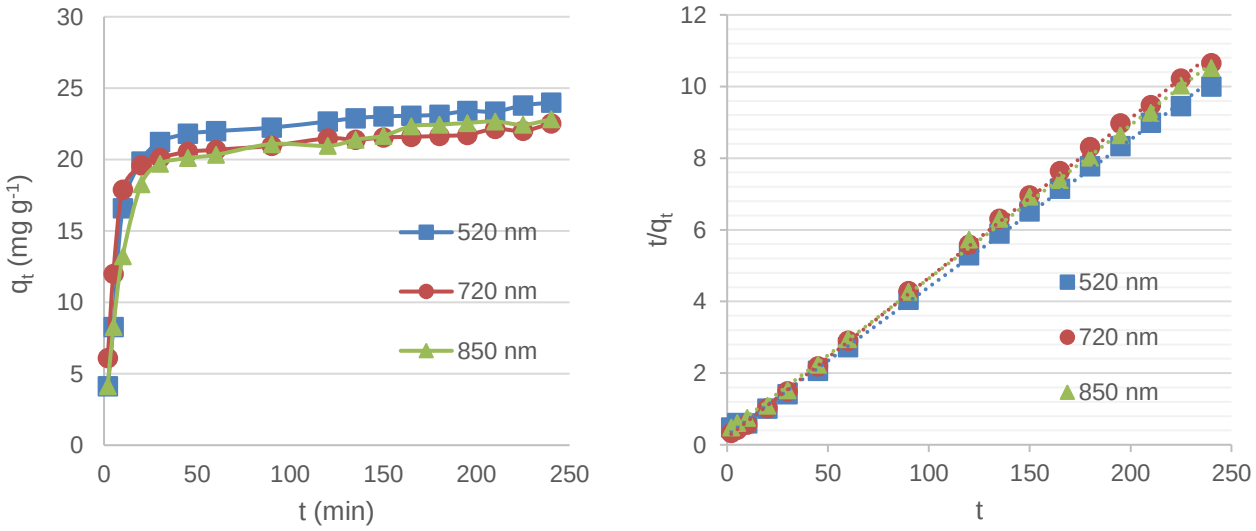

Figure 7. Left: Influence of fibre dimensions on the diffusion of L-tryptophan from electrospun webs into water. All samples prepared with14% w/v CA. (■) mean fibre diameter = 520 nm (flow rate: 0.002 ml min^{-1}, V: 25 kV); (●) mean fibre diameter = 720 nm (flow rate: 0.004 ml min^{-1}, V: 25 kV); (▲) mean fibre diameter = 850 nm (flow rate: 0.004 ml min^{-1}, V: 30 kV). Right: residual plots from application of pseudo-second order model (t/q_t vs. t).

Table 5. Kinetic data from diffusion of L-tryptophan in water from the electrospun webs with varying fibre diameter, at constant concentration of CA in spinning solution (14% w/v).

Fibre diameter (nm)	q_e (mg g^{-1})	$-h_0$ (mg g^{-1} min^{-1})	$-K_2$(mg g^{-1} min^{-1})	R^2
520	24.33	3.46	0.0058	0.999
720	22.47	4.84	0.0096	0.999
850	23.36	2.75	0.0050	0.999

It is interesting that in all kinetic data (Tables 4 and 5) both initial desorption and rate constant are highest for fibres with a mean fibre diameter of 720 nm, when it might have been expected that the greater surface area of thinner fibres would have led to a higher rate of diffusion. The diffusion distance and rate constant from the core to the surface of the fibre may be affected by the cross-sectional profile of the fibre [39]. Electrospun fibres are known to exhibit different fibre morphologies and profiles such as rounded, flat/ribbon or pitted [27]. A flat fibre will have a shorter distance from the centre to the surface along its width compared to a round fibre [39]. At high flow rates and/or high voltage, solvent evaporated quickly (beads and round fibres formed; see Figures 5a and 5c), phase-separation became difficult, and L-tryptophan remained inside the beads/round fibres where solvent was trapped, as has been previously observed [40]. Therefore, when the beads were dry, L-tryptophan was encapsulated inside. Consequently, potential increased retardation of L-tryptophan release from bead matrices may have caused the observed inconstancies in diffusion of L-tryptophan from fibres with evidence of bead formation [41,42].

4. Conclusions

A new ternary solvent system consisting of acetone: DMAc: methanol (2:1:2) has been demonstrated to permit the solution blending of CA with the water soluble amino acid, L-tryptophan. Nanofibrous webs that are substantially free of structural defects such as beads were continuously produced, producing fibres with diameters in the range 520-1,010 nm, depending on the process parameters. The morphology and diameter of fibres were influenced by the concentration of CA spinning solution, applied voltage and flow rates. Optimal CA concentration was 14%-16% w/v as judged by the ability to produce bead-free fibres using the ternary system. Fibres were readily produced at a high rate of production when the CA concentration was 14% w/v, voltage was 25 kV and the flow rate was 0.002 ml min^{-1}. However, at the higher flow rate of 0.004

ml min^{-1}, and as the voltage was progressively increased from 25 kV to 30 kV, some bead formation was in evidence. The kinetic release profile of L-tryptophan from electrospun CA nanofibres was described by the pseudo-second order kinetic model. Fibres with a mean fibre diameter of 720 nm provide both the highest initial desorption rate and rate constant. This was partially attributed to the low fibre diameter and high relative surface area, but also the fact that the fibres produced with a mean fibre diameter of 720 nm were the most bead-free, providing diffusion advantages over the fibres with the lowest mean fibre diameter (520 nm). The feasibility of combining L-tryptophan within fibres provides a promising route for manufacture of transdermal delivery devices.

5. Funding

This research did not receive any specific grant from funding agencies in the public, commercial, or not-for-profit sectors.

6. References

[1] M. Phiriyawirut, Gallic Acid-loaded Cellulose Acetate Electrospun Nanofibers: Thermal Properties, Mechanical Properties, and Drug Release Behavior, Open Journal of Polymer Chemistry (2012).
[2] W.K. Son, J.H. Youk, T.S. Lee, W.H. Park, Preparation of Antimicrobial Ultrafine Cellulose Acetate Fibers with Silver Nanoparticles, Macromolecular Rapid Communications 25(18) (2004) 1632-1637.
[3] P. Taepaiboon, U. Rungsardthong, P. Supaphol, Vitamin-loaded electrospun cellulose acetate nanofiber mats as transdermal and dermal therapeutic agents of vitamin A acid and vitamin E, Eur J Pharm Biopharm 67(2) (2007) 387-97.
[4] O. Suwantong, P. Opanasopit, U. Ruktanonchai, P. Supaphol, Electrospun cellulose acetate fiber mats containing curcumin and release characteristic of the herbal substance, Polymer 48(26) (2007) 7546-7557.
[5] K. Ohkawa, S. Hayashi, A. Nishida, H. Yamamoto, J. Ducreux, Preparation of Pure Cellulose Nanofiber via Electrospinning, Textile Research Journal 79(15) (2009) 1396-1401.
[6] X.M. Wu, C.J. Branford-White, L.M. Zhu, N.P. Chatterton, D.G. Yu, Ester prodrug-loaded electrospun cellulose acetate fiber mats as transdermal drug delivery systems, J Mater Sci Mater Med 21(8) (2010) 2403-11.
[7] T. Chantarodsakun, T. Vongsetskul, K. Jangpatarapongsa, P. Tuchinda, S. Uamsiri, C. Bamrungcharoen, S. Kumkate, P. Opaprakasit, P. Tangboriboonrat, [6]-Gingerol-loaded cellulose acetate electrospun fibers as a topical carrier for controlled release, Polymer Bulletin 71(12) (2014) 3163-3176.
[8] M. Gouda, A. Hebeish, A. Aljafari, Synthesis and characterization of novel drug delivery system based on cellulose acetate electrospun nanofiber mats, Journal of Industrial Textiles 43(3) (2014) 319-329.
[9] D.-G. Yu, X.-Y. Li, X. Wang, W. Chian, Y.-Z. Liao, Y. Li, Zero-order drug release cellulose acetate nanofibers prepared using coaxial electrospinning, Cellulose 20(1) (2013) 379-389.
[10] S. Tungprapa, I. Jangchud, P. Supaphol, Release characteristics of four model drugs from drug-loaded electrospun cellulose acetate fiber mats, Polymer 48(17) (2007) 5030-5041.
[11] S. Wongsasulak, M. Patapeejumruswong, J. Weiss, P. Supaphol, T. Yoovidhya, Electrospinning of food-grade nanofibers from cellulose acetate and egg albumen blends, Journal of Food Engineering 98(3) (2010) 370-376.

[12] H. Liu, Y.-L. Hsieh, Ultrafine fibrous cellulose membranes from electrospinning of cellulose acetate, Journal of Polymer Science Part B: Polymer Physics 40(18) (2002) 2119-2129.
[13] S. Tungprapa, T. Puangparn, M. Weerasombut, I. Jangchud, P. Fakum, S. Semongkhol, C. Meechaisue, P. Supaphol, Electrospun cellulose acetate fibers: effect of solvent system on morphology and fiber diameter, Cellulose 14(6) (2007) 563-575.
[14] L. Van der Schueren, B. De Schoenmaker, Ö.I. Kalaoglu, K. De Clerck, An alternative solvent system for the steady state electrospinning of polycaprolactone, European Polymer Journal 47(6) (2011) 1256-1263.
[15] Z. Ma, M. Kotaki, S. Ramakrishna, Electrospun cellulose nanofiber as affinity membrane, Journal of Membrane Science 265(1–2) (2005) 115-123.
[16] Z. Ma, S. Ramakrishna, Electrospun regenerated cellulose nanofiber affinity membrane functionalized with protein A/G for IgG purification, Journal of Membrane Science 319(1–2) (2008) 23-28.
[17] C. BELL, J. ABRAMS, D. NUTT, Tryptophan depletion and its implications for psychiatry, The British Journal of Psychiatry 178(5) (2001) 399-405.
[18] V. Pillay, C. Dott, Y.E. Choonara, C. Tyagi, L. Tomar, P. Kumar, L.C. du Toit, V.M.K. Ndesendo, A Review of the Effect of Processing Variables on the Fabrication of Electrospun Nanofibers for Drug Delivery Applications, Journal of Nanomaterials 2013 (2013) 22.
[19] W.K. Son, J.H. Youk, T.S. Lee, W.H. Park, Electrospinning of ultrafine cellulose acetate fibers: Studies of a new solvent system and deacetylation of ultrafine cellulose acetate fibers, Journal of Polymer Science Part B: Polymer Physics 42(1) (2004) 5-11.
[20] B. Ghorani, S.J. Russell, P. Goswami, Controlled Morphology and Mechanical Characterisation of Electrospun Cellulose Acetate Fibre Webs, International Journal of Polymer Science 2013 (2013) 12.
[21] D. Haas, S. Heinrich, P. Greil, Solvent control of cellulose acetate nanofibre felt structure produced by electrospinning, Journal of Materials Science 45(5) (2009) 1299-1306.
[22] B. Ghorani, P. Goswami, S.J. Russell, Parametric Study of Electrospun Cellulose Acetate in Relation to Fibre Diameter, Research Journal of Textile and Apparel 19(4) (2015) 24-40.
[23] L. Ghasemi-Mobarakeh, D. Semnani, M. Morshed, A novel method for porosity measurement of various surface layers of nanofibers mat using image analysis for tissue engineering applications, Journal of Applied Polymer Science 106(4) (2007) 2536-2542.
[24] M. Ziabari, V. Mottaghitalab, A.K. Haghi, Evaluation of electrospun nanofiber pore structure parameters, Korean Journal of Chemical Engineering 25(4) (2008) 923-932.
[25] S. Uday Kumar, I. Matai, P. Dubey, B. Bhushan, A. Sachdev, P. Gopinath, Differentially cross-linkable core-shell nanofibers for tunable delivery of anticancer drugs: synthesis, characterization and their anticancer efficacy, RSC Advances 4(72) (2014) 38263-38272.
[26] J.A. Sweeney, S.A. Asher, Tryptophan UV resonance Raman excitation profiles, The Journal of Physical Chemistry 94(12) (1990) 4784-4791.
[27] S. Koombhongse, W. Liu, D.H. Reneker, Flat polymer ribbons and other shapes by electrospinning, Journal of Polymer Science Part B: Polymer Physics 39(21) (2001) 2598-2606.
[28] S.L. Shenoy, W.D. Bates, H.L. Frisch, G.E. Wnek, Role of chain entanglements on fiber formation during electrospinning of polymer solutions: good solvent, non-specific polymer–polymer interaction limit, Polymer 46(10) (2005) 3372-3384.
[29] B. Ghorani, N. Tucker, Fundamentals of electrospinning as a novel delivery vehicle for bioactive compounds in food nanotechnology, Food Hydrocolloids 51 (2015) 227-240.
[30] K.H. Lee, H.Y. Kim, H.J. Bang, Y.H. Jung, S.G. Lee, The change of bead morphology formed on electrospun polystyrene fibers, Polymer 44(14) (2003) 4029-4034.
[31] G. Eda, S. Shivkumar, Bead structure variations during electrospinning of polystyrene, Journal of Materials Science 41(17) (2006) 5704-5708.
[32] S.H. Tan, R. Inai, M. Kotaki, S. Ramakrishna, Systematic parameter study for ultra-fine fiber fabrication via electrospinning process, Polymer 46(16) (2005) 6128-6134.
[33] J.-Y. Tseng, C.-Y. Chang, C.-F. Chang, Y.-H. Chen, C.-C. Chang, D.-R. Ji, C.-Y. Chiu, P.-C. Chiang, Kinetics and equilibrium of desorption removal of copper from magnetic polymer adsorbent, Journal of Hazardous Materials 171(1) (2009) 370-377.
[34] Y.S. Ho, G. McKay, A Comparison of Chemisorption Kinetic Models Applied to Pollutant Removal on Various Sorbents, Process Safety and Environmental Protection 76(4) (1998) 332-340.
[35] Y.S. Ho, G. McKay, Pseudo-second order model for sorption processes, Process Biochemistry 34(5) (1999) 451-465.
[36] S.J. Eichhorn, W.W. Sampson, Relationships between specific surface area and pore size in electrospun polymer fibre networks, J R Soc Interface 7(45) (2010) 641-9.

[37] G. Kim, H. Yoon, Y. Park, Drug release from various thicknesses of layered mats consisting of electrospun polycaprolactone and polyethylene oxide micro/nanofibers, Applied Physics A 100(4) (2010) 1197-1204.
[38] M. Chen, P.K. Patra, M.L. Lovett, D.L. Kaplan, S. Bhowmick, Role of electrospun fibre diameter and corresponding specific surface area (SSA) on cell attachment, J Tissue Eng Regen Med 3(4) (2009) 269-79.
[39] D.-G. Yu, Y. Xu, Z. Li, L.-P. Du, B.-G. Zhao, X. Wang, Coaxial Electrospinning with Mixed Solvents: From Flat to Round Eudragit L100 Nanofibers for Better Colon-Targeted Sustained Drug Release Profiles, Journal of Nanomaterials 2014 (2014) 8.
[40] J. Zeng, L. Yang, Q. Liang, X. Zhang, H. Guan, X. Xu, X. Chen, X. Jing, Influence of the drug compatibility with polymer solution on the release kinetics of electrospun fiber formulation, Journal of Controlled Release 105(1–2) (2005) 43-51.
[41] S.K. Jain, A. Jain, Y. Gupta, M. Ahirwar, Design and development of hydrogel beads for targeted drug delivery to the colon, AAPS PharmSciTech 8(3) (2007) E56.
[42] X.Z. Shu, K.J. Zhu, Controlled drug release properties of ionically cross-linked chitosan beads: the influence of anion structure, International Journal of Pharmaceutics 233(1–2) (2002) 217-225.